First-principles calculations of structural and mechanical properties of $YFeO_3$

TAO SHEN[a,*], YUE FENG[a], CHAO HU[a], HAILONG DAI[a], MINGXIN SONG[a], WENLONG YANG[a],
HONGCHEN LIU[b], XINLAO WEI[c]
[a]College of Applied Sciences, Harbin University of Science and Technology, 150080 Harbin, China
[b]School of Electrical Engineering and Automation, Harbin Institute of Technology, Harbin 150001, China
[c]Key Laboratory of Engineering Dielectrics and Its Application, Ministry of Education, Harbin University of Science and
Technology, 150080 Harbin, China

First principles calculations have been performed to investigate the structural and elastic properties of the *Pnma* orthorhombic $YFeO_3$. The GGA calculations overestimated the lattice constants, whereas LDA substantially underestimated them. The elastic constants, elastic moduli, Poisson's ratio and elastic anisotropy have been investigated. The elastic anisotropy and directional dependent Young's modulus of *Pnma* $YFeO_3$ are analyzed. $YFeO_3$ shows an elastic anisotropic behavior according to the universal elastic anisotropy index A^U = 0.7. The orthorhombic *Pnma* $YFeO_3$ is found to be ductile and mechanically stable at zero pressure and zero temperature.

1. Introduction

In recent years, an increasing attention has been given towards the study of the perovskite-type oxides because of their specific properties, e.g., ferroelectricity [1, 2], piezoelectricity [3, 4], multiferroic orthoferrite [5], and semiconductivity [6].

$RFeO_3$ (R=Y and rare earth) crystallizes in orthorhombic perovskite-type structure, and shows unique magnetic properties. The yttrium ferrite has gained special interest owing to the fact that orthorhombic $YFeO_3$ (space group *Pnma*) [7] is an attractive magnetic material at room temperature: antiferromagnetic below TN=644 (Néel temperature). The Y cation is nearly diamagnetic and the magnetic moments are due entirely to the Fe atoms. The magnetic properties can be effectively improved by doping with transition metals [8, 9]. These properties make $YFeO_3$ attracting great interest for promising application in magneto-optical devices and promote considerable experimental and theoretical researches, especially in thin-films cases [10-12]. The study of material properties such as structural properties and elastic constants is significant in practical applications. But little research on the elastic constants of $YFeO_3$ was reported, which limits the fundamental understanding and fabrication of $YFeO_3$, e.g., the strain energy estimation [13] and stress analysis [14] in epitaxial thin films. The dearth of mechanical properties in $YFeO_3$ therefore motivates the present research.

To the best of our knowledge, first-principles calculation is known to be a useful tool to investigate the properties of the material. A theoretical investigation of the structural and mechanical properties is valuable and may serve as a guide for eventual technological applications. In my present work, we present the first-principles study of the structural and elastic properties of the $YFeO_3$, by using the density functional theory (DFT) with Ultrasoft Pseudoptentials (USP). Our paper is arranged as follows: In section 2, we detail the computational method. In section 3, we specifically discuss the results of our calculated structural and elastic properties. Finally, the conclusions are summarized in section 4.

2. Computational method

The first principles calculations of antiferromagnetic materials $YFeO_3$ have been performed using the DFT implemented in the Cambridge Serial Total Energy (CASTEP) code [15]. We used the Materials Visualizer to build the $YFeO_3$ model. The model of $YFeO_3$ is shown in Fig. 1. In our calculation, the orthorhombic $YFeO_3$ cell consists of 20 atoms, and all of the Fe atoms are at the center of FeO_6 octahedra. Ultrasoft pseudopotentials (USP) were introduced by Vanderbilt [16, 17]. On the basis, we treated explicitly 11 valence electrons for Y $(4s^2 4p^6 4d^1 5s^2)$, 6 for oxygen $(2s^2 2p^4)$, and 14 for Fe $(3p^6 3d^6 4s^2)$. The exchange-correlation is treated within the

generalized gradient approximation (GGA), developed by Perdew, Burke, and M. Ernzerhof (PBE) [18]. Additionally, the CA-PZ [19] functions of LDA were also used for comparison. Integration over the Brillouin zone can be simplified by discrete summation over a small number of special points using the Monkhorst-Pack method [20]. In addition, symmetry considerations suggest that only k-points within the irreducible segment of the Brillouin zone should be taken into account. The Broyden-Fletcher-Goldfarb-Shenno (BFGS) minimization scheme was used to determine the structural parameters. The threshold for the converged procedure is that: a total energy convergence of 0.5×10^{-6} eV/atom, Hellmann-Feynman ionic force of 0.01 eV/Å, maximum stress of 0.02 Pa, and maximum displacement of 0.5×10^{-3} Å.
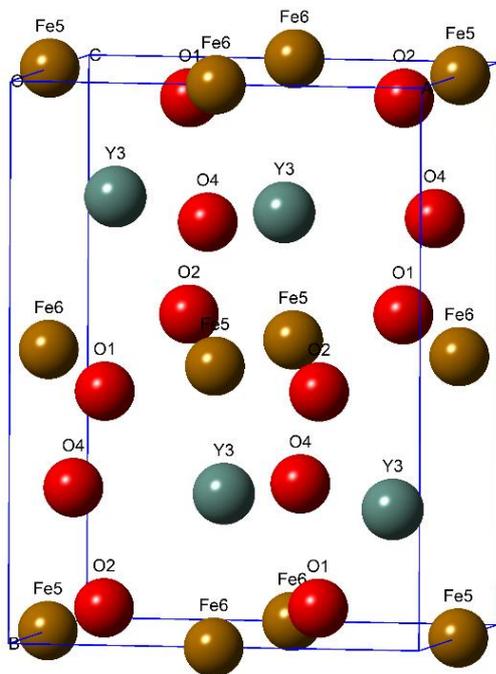
Fig. 1. The primitive cell crystal structure of the orthorhombic YFeO₃

3. Results and discussion

3.1 Structural properties

The lattice parameters of YFeO₃ obtained from the full structural optimization using the LDA and GGA functional are listed in the Table 1. The lengths and cell volume are usually underestimated by a few percent. As shown in Table 1, the structural parameters obtained from LDA have about 12% underestimation of the equilibrium volume compared with the average experimental values. The GGA functional provides a better overall description of the electronic subsystem than the LDA functional. GGA revises the underestimation but may underbind instead. As

shown in Table 1, the results acquired from GGA are in agreement with experimental mean values [21], which have an average 1.7% overestimation of the lattice constants (a, b and c). According to the discussions above, the GGA is suitable to describe the structure of orthorhombic YFeO₃. For simplicity, the following discussions are focused on the GGA results.

Table 1. The lattice constants (a, b, c in Å and V in Å³), single crystal elastic constants (C_{ij} in GPa), shear modulus, Young's modulus (E in GPa), Poissions's ratio (σ) and anisotropic factors of YFeO₃.

Method	GGA	LDA	Exp.[a]
a	5.75	5.44	5.5946
b	7.65	7.23	7.6056
c	5.37	5.02	5.2817
V	236.21	197.44	224.74
C_{11}	218.88	-	-
C_{22}	312.12	-	-
C_{33}	275.46	-	-
C_{44}	80.55	-	-
C_{55}	65.73	-	-
C_{12}	111.74	-	-
C_{13}	170.47	-	-
C_{23}	160.40	-	-
B_{V}	200.27	-	-
B_{R}	194.01	-	-
B_{H}	197.14	-	-
G_{V}	72.177	-	-
G_{R}	63.66	-	-
G_{H}	67.91	-	-
E	182.76	-	-
σ	0.34	-	-
A_{1}	1.866	-	-
A_{2}	1.04	-	-
A_{3}	2.35	-	-
A^{U}	0.70	-	-
A_{B}	0.02	-	-
A_{G}	0.06	-	-

[a] [21]

3.2 Elastic constants

The elastic stiffness tensor is related to the stress tensor and the strain tensor from Hooke's law. In the most general case, the elastic stiffness tensor has only the 21 non-zero independent components due to the symmetry of the stress tensor and strain tensor. For an orthorhombic crystal, the symmetrical elements are reduced from twenty-one to nine (C_{11}, C_{22}, C_{33}, C_{44}, C_{55}, C_{66}, C_{12}, C_{13} and C_{23}). The elastic stiffness coefficients are determined from the applied stress to the computed strain [22]. In Table 1, we show the elastic constants calculated from the GGA functional. Because there is no previous study for the mechanical properties of YFeO₃ using calculations or

experiments, our results may serve as a predictive study. The mechanical stability criteria for orthorhombic YFeO$_3$ are:

$$\left(C_{22}+C_{33}-2C_{23}\right)>0$$
$$\left(C_{11}+C_{22}+C_{33}+2C_{12}+2C_{13}+2C_{13}\right)>0 \quad (1)$$
$$C_{11}>0, \quad C_{22}>0, C_{33}>0, C_{44}>0, C_{55}>0, C_{66}>0.$$

Our results for the elastic constants in Table 1 satisfy all of these conditions and indicate that YFeO$_3$ is mechanically stable. The elastic constants C_{11}, C_{22} and C_{33} describe the elasticity in length. The elastic constants C_{12}, C_{13}, C_{23}, C_{44}, C_{55} and C_{66} describe the elasticity in shape.

In orthorhombic crystals, C_{11}, C_{22} and C_{33} also denote atomic characteristics between adjacent atomic planes. Table 1 shows that C_{22} is much greater than C_{11} and C_{33}. Additionally, for the orthorhombic YFeO$_3$, the unit cell is elongated along the b-axis. These results indicate that the atomic bonds along the {0 1 0} plane between the nearest neighbors are stronger than the {1 0 0} and the {0 0 1} plane, and the b-axis is least compressible. Furthermore, we may infer that the cell parameters a, c are more sensitive to the pressure and temperature than the parameter b. Furthermore, the shear constants C_{11} (C_{22} and C_{33}) and elastic constants C_{44} (C_{55} and C_{66}) represent the unidirectional compression along the crystalline directions and the resistance to shear deformation, respectively. The values of the C_{11} (C_{22} and C_{33}) are much greater than the elastic constants C_{44} (C_{55} and C_{66}), which indicates that the resistance to unidirectional compression is much weaker than resistance to shear deformation.

3.3 Elastic moduli

The theoretical polycrystalline elastic modulus can be determined from the independent elastic constants above. We calculated the polycrystalline modulus using the Voigt [23] and Reuss [24] method. For orthorhombic YFeO$_3$, the Reuss (B_R, G_R) and Voigt (B_V, G_V) bulk moduli and shear moduli are expressed by [25]

$$B_V = (1/9)\left[C_{11}+C_{12}+C_{33}+2\left(C_{12}+C_{13}+C_{23}\right)\right]$$
$$B_R = 1/\left[\left(S_{11}+S_{22}+S_{33}\right)+2\left(S_{12}+S_{13}+S_{23}\right)\right] \quad (2)$$

The Voigt Shear modulus (G_V) and the Reuss bulk modulus (G_R) are determined as:

$$G_V = (1/15)\left[C_{11}+C_{22}+C_{33}+3(C_{44}+C_{55}+C_{66})-(C_{12}+C_{13}+C_{23})\right]$$
$$G_R = 15/[4(S_{11}+S_{22}+S_{33})-4\left(S_{12}+S_{13}+S_{23}\right)+3(S_{44}+S_{55}+S_{66})]$$
$$(3)$$

S_{ij} are the elastic compliance constants:

$$S_{11}=\left(C_{22}C_{33}-C_{23}^2\right)/\Delta, S_{22}=\left(C_{11}C_{33}-C_{13}^2\right)/\Delta, S_{33}=\left(C_{11}C_{22}-C_{12}^2\right)/\Delta$$
$$S_{12}=\left(C_{13}C_{23}-C_{12}C_{23}\right)/\Delta, S_{13}=\left(C_{12}C_{23}-C_{13}C_{22}\right)/\Delta, S_{23}=\left(C_{12}C_{13}-C_{11}C_{23}\right)/\Delta$$
$$(4)$$

$S_{ii}=1/C_{ii}$ (i=4, 5, 6), where Δ is defined as:

$$\Delta = C_{13}\left(C_{12}C_{23}-C_{13}C_{22}\right)+C_{23}\left(C_{12}C_{13}-C_{23}C_{11}\right)$$
$$+C_{33}\left(C_{11}C_{12}-C_{12}^2\right) \quad (5)$$

The Voigt-Reuss-Hill (VRH) averages for the bulk modulus (*B*) and shear modulus (*G*) are:

$$B=1/2\left(B_R+B_V\right), G=1/2\left(G_R+G_V\right) \quad (6)$$

$$E=9BG/(3B+G), \sigma=(3B-2G)/\left[2(3B+G)\right] \quad (7)$$

Using the method described above, the Young's modulus *E*, shear modulus *G*, Poisson's ratio σ and bulk modulus *B* for *Pnma* YFeO$_3$ at zero temperature are calculated by GGA. These results are listed in Table 1. Bulk modulus *B* serves as a measurement of the resistance of a crystal to a volumetric changing. Additionally, a larger bulk modulus also means a shorter bond length between adjacent atoms.

The high value for the calculated bulk modulus indicates that the material does not undergo any volumetric deformation and, therefore, is incompressible. Through comparison with the results obtained by other researchers, we find that the average Y-O bond length (2.40 Å) of orthorhombic *Pnma* YFeO$_3$ is shorter than the Y-O bond length (2.51 Å) of YAlO$_3$, which indicates that the YAlO$_3$ possesses a smaller bulk modulus (*B*=150) [26].

To predict the brittle and ductile behavior of the solid, Pugh [27] introduced the ratio of bulk modulus to the shear modulus of the polycrystalline phases (*B/G*), which is related to the brittle or ductile characteristics of the material. If *B/G* > (<) 1.75, the crystal behaves in a ductile (brittle) manner. The other condition for being brittle or ductile, which is derived from Pugh's criterion for *B/G* is that, when σ is less than 0.26, the material is brittle; otherwise, it is ductile. For orthorhombic *Pnma* YFeO$_3$, *B/G* is 2.8 and σ is 0.34; therefore, the material is ductile.

The Poisson's ratio also reflects the volume change during elastic deformation [28]. It describes the stability of a crystal against the shear stress. If the σ reaches to 0.5, no volumetric deformation occurs.

3.4 Elastic anisotropy

The anisotropic behavior is an important property that describes the different atomic arrangements along different directions. Anisotropic behavior has an important implication in engineering science as well as in crystal physics. The Zener anisotropic factors in orthorhombic phase are given as follows:

$$A_1 = 4C_{44} / \left(C_{11} + C_{33} - 2C_{13} \right) A_2 = 4C_{55} / \left(C_{22} + C_{33} - 2C_{33} \right)$$
$$A_3 = 4C_{66} / \left(C_{11} + C_{22} - 2C_{12} \right)$$

(8)

The anisotropic factor $A1$ expresses the shear anisotropic factor for the {1 0 0} shear plane in the {0 1 1} and {0 1 0} directions and $A2$ expresses the shear anisotropic factor for the {0 1 0} shear plane in the {1 0 1} and {0 0 1} directions. Finally, $A3$ describes the shear anisotropic factor in the {0 0 1} shear plane in the {1 1 0} and {0 1 0} directions.

The anisotropic shear factors obtained from the theoretical studies are given in Table 1. For an isotropic crystal, the values of the factors $A1$, $A2$, and $A3$ must be equal to one, while any departure from unity attributes to the elastic anisotropy. Table 1 shows that the value of $A2$ obtained from GGA approaches to one, which indicates that the {0 1 0} shear planes shows isotropic in the {1 0 1} and {0 0 1} directions. For $A1$ and $A2$, the large divergence from one indicates that the {0 1 0} shear planes in the {1 0 1} and {0 0 1} directions and the {0 0 1} shear planes in the {1 1 0} and {0 1 0} directions have anisotropic behavior.

Shivakuma and Martin [29] presented a universal anisotropic index, A^{U}, to quantity the elastic anisotropy of all types of single crystals.

$$A^{\mathrm{U}} = 5G_V / G_R + B_V / B_R - 6 \qquad (9)$$

A^{U} is zero for locally isotropic single crystals. Any departure of the value from zero describes the extent of the single crystal anisotropy, and unlike other methods, it considers both the shear and the bulk contributions.

Alternatively, Chung and Buessem [30] proposed a concept of percentage elastic anisotropy, which is a measure of elastic anisotropy possessed by the crystal. The percentage anisotropy is expressed by

$$A_B = \left(B_V - B_R \right) / \left(B_V + B_R \right), A_G = \left(G_V - G_R \right) / \left(G_V + G_R \right)$$
(10)

For equations above, a value of 1 is the largest possible is maximum possible anisotropy; while a value of zero is associated with elastic isotropy. The calculated anisotropy index A^{U}, A_B and A_G of *Pnma* YFeO$_3$ are listed in Table 1. The departure of A^{U} from zero and the calculated A_B and A_G demonstrate that orthorhombic YFeO$_3$ is anisotropic in its elastic behavior.

Additionally, the dependence of reciprocal of Young's modulus on crystallographic direction represented by a three-dimensional curved surface can denote the elastic anisotropy of a system. The direction dependent Young's modulus for orthorhombic system is expressed as [31]:

$$1/E = S_{11}l_1^4 + 2S_{12}l_1^2l_2^2 + 2S_{13}l_1^2l_3^2 + S_{22}l_2^4 + 2S_{23}l_2^2l_3^2 + S_{33}l_3^4$$
$$+ S_{44}l_2^2l_3^2 + S_{55}l_1^2l_3^2 + S_{66}l_1^2l_2^2 ,$$

(11)

where S_{ij} are the elastic compliance constants, and l_1, l_2 and l_3 are the directional cosines to the X, Y and Z axis. The direction dependent Young's modulus for orthorhombic YFeO$_3$ are shown in Fig. 2. The three-dimensional closed surface is determined by Eq. (11), and the Young's modulus in a given direction corresponds to the distance from the origin of coordinate to the surface. As shown in Fig. 2, the distorted sphere implies the extent of elastic anisotropy. The Young's modulus in different planes (projection of the elastic modulus on XY, XZ and YZ) for orthorhombic YFeO$_3$ is plotted in Fig. 3. The bonding features between the different adjacent planes and inter-layer anisotropy can be revealed from the projection.

4. Conclusion

The structural and mechanical properties of *Pnma* orthorhombic YFeO$_3$ have been investigated using the first principles within GGA and LDA. My results are shown as follows: (1) The GGA calculations of the structural parameters are in good agreement with the experimental values, while LDA largely underestimated them. (2) The *Pnma* YFeO$_3$ is found to be mechanically stable at zero pressure and zero temperature. (3) The calculated Poisson's ratio of orthorhombic *Pnma* YFeO$_3$ is small, and it indicates that YFeO$_3$ is relatively stable against shear. (4) For the YFeO$_3$ compound, the B/G is larger than 1.5, and thus YFeO$_3$ is thought to be ductile material. (5) The orthorhombic *Pnma* YFeO$_3$ is incompressible and anisotropic.
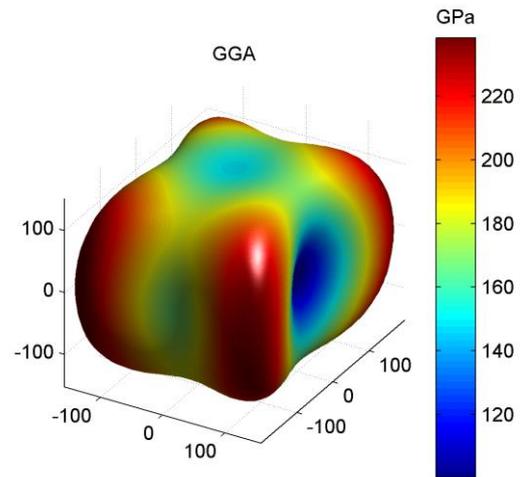
Fig. 2. Direction dependence of Young's modulus (GGA results) in Pnma YFeO$_3$.
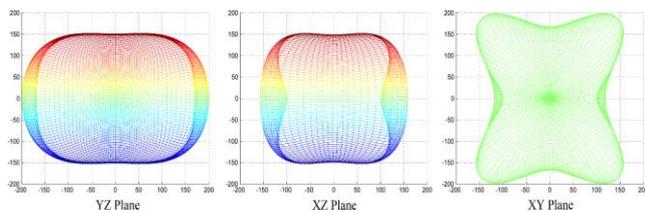
*Fig. 3. The projection of Young's modulus
(GGA results) in different planes for Pnma YFeO₃.*

Acknowledgements

References

[1] L. Li, M. Zhang, P. Tian, W. Gu, X. Wang, Ceram. Int. **40**, 13813 (2014).

[2] K. Qian, B. J. Fang, Q. B. Du, J. N. Ding, X. Y. Zhao, H. S. Luo, Phys. Status Solidi A, **210,** 1149 (2013).

[3] B. J. Fang, N. Jiang, J. N. Ding, Phys. Status Solidi A, **209**, 1239 (2012).

[4] H. Wang, B. Wang, Q. Li., Z. Zhu, R. Wang, C. H. Woo, Phys. Rev. B **75**, 245209 (2007).

[5] Y. Tokunaga, Y. Taguchi, T. Arima, Y. Tokura, Phys. Rev. Lett. **112**, 037203 (2014).

[6] H. P. R. Frederikse, W. R. Hosler, Phys. Rev. A **134**, 442 (1964)

[7] B. D. Boulay, E. N. Maslen, V. A. Streltsov, Acta Crystallogr. Sect. B: Struct. Sci. **51**, 921 (1995).

[8] H. Shen, J. Y. Xu, M. Jin, G. J. Jiang, Ceram. Int. **38**, 1473 (2012).

[9] X. Yuan, Y. Sun, M. X. Xu, Ceram. Int. **196**, 362 (2012).

[10] J. Scola, W. Noun, E. Popova, A. Fouchet, Y. Dumont, N. Keller, Phys. Rev. B **81**, 174409 (2010).

[11] J. Scola, P. Boullay, W. Noun, E. Popova, Y. Dumont, A. Fouchet, N. Keller, J. Appl. Phys. **110**, 043928 (2011).

[12] S. J. Ahn, J. H. Lee, Y. K. Jeong, E. H. Na, Y. M. Koo, H. M. Jang, Mater. Chem. Phys. **138**, 929 (2013).

[13] T. Gressmann, U. Welzel, A. Leineweber, E. J. Mittemeijer, Z. K. Liu, Acta Mater. **55**, 5833 (2007).

[14] J. Y. Shen, S. Johnston, S. L. Shang, T. Anderson, J. Cryst. Growth **240**, 6 (2002).

[15] M. D.Segall, P. J. D. Lindan, M. J. Probert, J. Phys.: Condens. Matter. **14**, 2717 (2002).

[16] D. Vanderbilt, Phys. Rev. B **41**, 7892 (1990).

[17] G. Kresse, J. Hafner, J. Phys.: Condens. Matter **6**, 8245 (1994).

[18] J. P. Perdew, K. Burke, M. Ernzerhof, Phys. Rev. Lett. **77**, 3865 (1996).

[19] D. M. Ceperly, B. J. Alde, Phys. Rev. Lett. **45**, 566 (1980).

[20] H. J. Monkhorst, J. D. Pack, Phys. Rev. B **13**, 5188 (1976).

[21] H. Shen, J. Y. Xu, A. H. Wu, J. T. Zhao, M. L. Shi, Mater. Sci. Eng. B **157**, 77 (2009).

[22] B. B. Karki, L. Stixrude, S. J. Clark, M. C. Warren, G. J. Ackland, J. Crain, Am. Mineral. **82**, 51 (1997).

[23] K. Tsubouchi, N. Mikoshiba, IEEE Trans. Sonics Ultrason. **32**, 634.

[24] A. Reuss, Z. Angew, Math. Meth. **9**, 49 (1929).

[25] O. Beckstein, J. E. Klepeis, G. L. W. Hart, O. Pankratov, Phys. Rev. B, **63**, 134112 (2001).

[26] Z. C. Huang, J. Feng, W. Pan, Comput. Mater. Sci, **50**, 3056 (2011).

[27] S. F. Pugh, Philos. Mag. Series **7** 45, 823 (1954).

[28] P. Ravindran, L. Fast, P. A. Korzhavyi, B. Johansson, J. Wills, O. Eriksson, J. Appl. Phys. **84**, 4891 (1998).

[29] I. R. Shivakumar, O. S. Martin, Phys. Rev. Lett. **101**, 055504 (2008).

[30] D. H. Chung, W. R. Buessem, J. Appl. Phys. **38**, 2010 (1967).

[31] J. F. Nye, Physical properties of Crystals, (Oxford: Clarendon Press, 1964).

———————————
*Corresponding author: taoshenchina@163.com